The inner structure of Zeldovich' pancakes

E. Aurell [1,2,3]*, D. Fanelli [3,4]†, S.N. Gurbatov [5,6] ‡ & A.Yu. Moshkov [5]§

February 2, 2008

[1] SICS, Box 1263, SE-164 29 Kista, Sweden
[2] NORDITA, Blegdamsvej 17, DK-2100 Copenhagen, Denmark
[3] Department of Numerical Analysis and Computer Science, KTH, S-100 44 Stockholm, Sweden
[4] Department of Cell and Molecular Biology, Karolinska Institute, SE-17177 Stockholm, Sweden
[5] Radiophysics Department, University of Nizhny Novgorod, 603600, Gagarina Av. 23, Russia, (permanent address)
[6] Observatoire de la Côte d'Azur, Lab. G.D. Cassini, B.P. 4229, F-06304 Nice Cedex 4, France.

Abstract

The evolution of a planar perturbation in a Einstein-de Sitter Universe is studied using a previously introduced Lagrangian scheme. An approximate discrete dynamical system is derived, which describes the mass agglomeration process qualitatively. Quantitative predictions for the late density profile are obtained therefrom, and validated by numerical simulations. The main result is a scaling regime for the density profile of a collapsing object of mass M around cosmological coordinate r^*, $\rho(r) \sim \frac{M}{d}\left(\frac{|r-r^*|}{d}\right)^{-\frac{1}{4}}$. The characteristic scale

*e-mail: eaurell@sics.se
†e-mail: fanelli@et3.cmb.ki.se
‡e-mail: gurb@rf.unn.ru
§e-mail: moshkov@rf.unn.ru

of the agglomeration, $d \sim (t/t_0)^{\frac{4}{9}}$, is an increasing function of cosmological time t. The major part of the mass hence always lies in a region with decreasing mass density. This shows that one-dimensional self-gravitating motion is not sufficient to effectively drive structure formation in an Einstein-de Sitter Universe. These results are compared with analogous investigations for the adhesion model (Burgers equation with positive viscosity), where the agglomeration is faster, and one-dimensional dynamics is effective. We further study the mutual motion of two mass agglomerations, and show that they oscillate around each other for long times, like two "heavy particles". Individual particles in the two agglomerations do not mix effectively on the time scale of the interagglomeration motion.

PACS numbers: 02.50.Ey, 05.60.-k,
Keywords: Self-gravitating dynamics; Mass density; Adhesion model; Burgers equation

1 Introduction

Structure formation in the Universe is a rich and challenging problem, which touches many sides of Physics. It is generally believed that the presently observed large scale structures have been generated by the process of the gravitational instability, acting on initially small density perturbations. The temperature fluctuations on the uniform Cosmic Microwave Background (CMB) radiation provide an image of these fluctuations, which were the seeds of the present large scale distribution of matter [6, 7, 2]. The observed CMB angular power spectrum is dominated by a peak at 1 degree of arc, and also shows structures at smaller scales.

According to present consensus, the constituents of our Universe are ordinary matter (5%), dark matter (25%) and dark energy (70%). The three forms can be summarily classified by how their energy densities change with a cosmic scale factor a: ordinary and dark matter behave as a^{-3}, radiation, which interacts with ordinary matter, behaves as a^{-4}, while dark energy, at least in the simplest models thereof, is independent of a. Hence, even if dark energy dominates today, dark matter and ordinary matter dominated earlier. Further, the Universe is flat, in agreement with an early epoch of

inflation. Within that scenario, the primordial density perturbations were random Gaussian with power spectrum $P(k) \sim Ak$, which is also consistent with the data. The ordinary matter content can be deduced from observations at e.g. visible or radio frequencies. The presence of dark matter can be inferred from the observed dynamics of cosmic objects, particularly from fast rotation of hydrogen clouds far outside the luminous disc of spiral galaxies, as well as high-velocity dispersion of galaxies in clusters [29]. Dark energy, or quintessence [5], is equivalent to a non-zero cosmological constant, Λ, in Einstein's equations [29], and there is recent support for a non-zero Λ also from redshift observations. All of these direct measurements can be compared with theoretical cosmology and the observed angular structure of the CMB. A sequence of peaks should indeed arise from coherent acoustic oscillations in the baryon-photon fluid during an early epoch. Their amplitudes and relative positions provide another series of tests of cosmological models, and put a different series of constraints on the parameters of such models, c.f. [26] for a recent review.

The growth of small initial perturbations to large-scale structures is essentially a problem in classical gravitational physics, where all the above mainly enters in the initial conditions, and the how the Universe expands as a whole. The problem is nevertheless far from trivial. A principal difficulty is that a self-gravitational medium has no ground-state, and the dynamics is not ergodic. Contrary to e.g. molecular dynamics, one cannot appeal to a shadowing lemma, and argue that even if a simulation only solves the equations of motion in a rough approximation, the simulated system nevertheless stays close to the real system, with different initial conditions. The single most influential result in structure formation, Zeldovich' pancake theory, was indeed developed without any recourse to simulation at all, but purely by extending linear analysis into the non-linear domain. The fact that this model and the adhesion model are still the benchmarks today shows the difficulty of firmly establishing the detailed characteristics of the mass agglomeration process.

The goal of this paper is to investigate the non-linear regime of the gravitational instability in the special case that the initial perturbations are planar. We also assume an Einstein-de Sitter Universe, and hence disregard the dark energy component. With these limitations, one can introduce a Lagrangian integration scheme, called the Quintic (Q) model [1, 10], which is both fast,

and exact from collision to collision. It is worth stressing that the Q model is just one of the possible representation of the dynamics [10]. A conceptually equivalent formulation was previously proposed by [27]. These two approaches share the characteristic that they allow to avoid sources of additional errors, like truncation, involved in any approximate numerical scheme (see [8]).

The focus is here on the inner structure of a pancake. The novelty with respect previous investigations [8, 27] is that, by making use of a discrete map to approximate the exact Q dynamics, we derive a close analytical expression for the density profile. These results are validated by direct numerical simulation, and compared with analogous results for the adhesion model. We further investigate the pair-wise motion of two pancakes under their mutual attraction.

The paper is organized as follows: in Section 2 we present the general background, and in Section 3 we re-derive, for completeness, the Q model. In Section 4 the evolution of a two particle system is considered: an approximate discrete system is derived and validated by numerical investigations. The analysis is extended in Section 5 where the inner structure of a single cluster is investigated. Improving previous results in [10] we establish the density profile of a collapsing cluster. In Section 6 we study the dynamics of two massive clusters, and in Section 7 we sum up and discuss our results.

2 From Vlasov-Poisson equations to the adhesion model

The evolution of collision-less dark matter in a three dimensional expanding Universe is described by the kinetic Vlasov-Poisson equations. Assume an inertial reference frame, and label the position with $\mathbf{r}$. Then it is customary to introduce the co-moving coordinate $\mathbf{x}$ by the following transformation [21]:

$$\mathbf{r} = a(t)\mathbf{x} \ , \tag{1}$$

where the scale factor $a(t)$ is function of proper world time. For an Einstein-de Sitter Universe

$$a = \left(\frac{t}{t_0}\right)^{2/3} \ , \tag{2}$$

where $t_0^{-2} = 6\pi G\rho(t_0)$, $\rho(t_0)$ is the homogeneous density at time t_0 [21, 29] and G is the gravitational constant. The Vlasov-Poisson equations then read:

$$\begin{cases} \partial_t f + \dfrac{\mathbf{p}}{ma^2} \cdot \nabla_{\mathbf{x}} f - \nabla_{\mathbf{x}} \psi \cdot \nabla_{\mathbf{p}} f = 0 \\ \\ \nabla^2 \psi = 4\pi G a^2 \left(\rho - \rho_b\right) , \end{cases} \tag{3}$$

where $\mathbf{p}$ is the variable conjugated to $\mathbf{x}$; $f(\mathbf{x}, \mathbf{p}, t)$ is the distribution function in the six-dimensional phase space $(\mathbf{x}, \mathbf{p})$; ψ is the gravitational potential and ρ_b is the mean mass density. The particle density $\rho(\mathbf{x}, t)$ and velocities $\mathbf{u}(\mathbf{x}, t)$ are given, in term of $f(\mathbf{x}, \mathbf{p}, t)$, as:

$$\rho(\mathbf{x}, t) = \frac{m}{a^3} \int f(\mathbf{x}, \mathbf{p}, t) d\mathbf{p} , \tag{4}$$

$$\rho(\mathbf{x}, t)\mathbf{u}(\mathbf{x}, t) = \frac{1}{a^4} \int \mathbf{p} f(\mathbf{x}, \mathbf{p}, t) d\mathbf{p}. \tag{5}$$

It is well known, see e.g. [28], that (3) admit special solutions of the form

$$f(\mathbf{x}, \mathbf{p}, t) = \frac{a^3 \rho(\mathbf{x}, t)}{m} \delta^d(\mathbf{p} - ma\mathbf{u}(\mathbf{x}, t)) , \tag{6}$$

where d is the dimension of space and $\delta^d(.)$ the d-dimensional delta function. We will refer to this class as to single-speed solutions, because to each given $(\mathbf{x}, t)$ corresponds a well defined velocity $\mathbf{u}$. Assuming (6), a closed system on the hydrodynamic level can be derived using (4) and (5):

$$\begin{cases} \partial_t \rho + 3\dfrac{\dot{a}}{a}\rho + \dfrac{1}{a}\nabla \cdot (\rho \mathbf{u}) = 0 \\ \\ \partial_t \mathbf{u} + \dfrac{\dot{a}}{a}\mathbf{u} + \dfrac{1}{a}(\mathbf{u} \cdot \nabla)\mathbf{u} = \mathbf{g} \\ \\ \nabla \cdot \mathbf{g} = -4\pi G a(\rho - \rho_b) , \end{cases} \tag{7}$$

where we have introduced $\mathbf{g} = -\nabla\psi/a$ such that $\nabla \times \mathbf{g} = 0$. It should be stressed that system (7) is valid as long as the distribution function $f(\mathbf{x}, \mathbf{p}, t)$ is in the form (6). Beyond the time of caustic formation, when fast particles cross slow ones, the solution becomes multi-stream. Hence, the pressure-less

and dissipation-less hydrodynamical equations of (7) are incomplete.

An ansatz that permits further progress is the so-called *condition of parallelism* which requires that the peculiar velocity is a potential field, that remains parallel to the gravitational peculiar acceleration field [21, 28, 4]:

$$\mathbf{g} = F(t)\mathbf{u} \tag{8}$$

The important assumption, in the present discussion, is that the proportionality $F(t)$ is space-independent. That can only strictly be true in the linear regime, where

$$F(t) = 4\pi G\rho_b b/\dot{b} \ , \tag{9}$$

and b is the amplitude of the perturbation. A natural further assumption is that only the linearly growing mode is excited [21, 4], which gives $b \sim t^{\frac{2}{3}}$ in our case. Defining the new velocity field $\mathbf{v} = \mathbf{u}/(a\dot{b})$, system (7) reduces to free motion in Eulerian coordinates

$$\partial_b \mathbf{v} + (\mathbf{v}\cdot\nabla)\mathbf{v} = 0 \ , \tag{10}$$

This is Zeldovich' pancake model in the original formulation [25]. It is also to referred as the Zeldovich approximation, because the contribution of the decaying mode of the density field has been neglected. The ansatz that the condition of parallelism holds also in the multi-stream region could be approximatively true, but is still a bold assumption to make.

After caustic formation one may think that the resulting change in the gravitational force could be modeled by an effective diffusive term. In the adhesion model, [15, 13], one hence introduces a term of the form $\nu\nabla^2\mathbf{v}$ in the right hand side of the equation (10):

$$\begin{cases} \partial_b \mathbf{v} + (\mathbf{v}\cdot\nabla)\mathbf{v} = \nu\nabla^2\mathbf{v} \\ \\ \mathbf{v} = -\nabla\tilde{\psi} \\ \\ \partial_b \rho + \nabla\cdot(\rho\mathbf{v}) = 0 \ , \end{cases} \tag{11}$$

where $\tilde{\psi} = \psi/(\dot{b}F(t))$. In order for the diffusion term to have a smoothing effect only in those regions where the particles crossing takes place, the phenomenological viscosity parameter ν should be small.

Although numerical experiments suggest qualitative agreement, the exact relationship between (3) and (11) is still an open problem. In a recent paper [10] a derivation of (11) was outlined in one dimension. Comparisons with numerical results suggested however that at least the diffusion term should be modified, to give instead transport equation in the class recently studied by Buchert and co-workers [3, 4]. We will here study the system (3) directly, and establish the inner structure of a mass agglomeration without the ansatz of parallelism.

3 The Q model, and its relation to the Zeldovich approximation and the adhesion model

We will consider the evolution of the one-dimensional perturbation in the expanding three dimension Universe, using the discrete approximation of initial condition. Let us assume, that in some interval L along the axis x all the matter is concentrated in the N sheets, which we will from now on call particles.

The Newtonian equations of motion for such N particles, interacting via gravity, follow from the Lagrangian [21]:

$$\mathcal{L} = \sum_i \frac{1}{2} m_i \dot{r_i}^2 - m_i \phi(r_i, t) \ , \tag{12}$$

where $\nabla_r^2 \phi = 4\pi G \rho$. In the point particle picture the density profile reads:

$$\rho(x_i, t) = \sum_{x_j} m_j a^{-3} \delta(x_i - x_j) \ , \tag{13}$$

where x_i is the co-moving coordinate of the i'th particle, in the direction of which the density and velocities vary.

Expressing (12) as a function of the proper coordinate, x_i, and assuming (13), the equation of motion of the i'th particle reads:

$$\frac{d^2 x_i}{dt^2} + 2\frac{\dot{a}}{a}\frac{dx_i}{dt} - 4\pi G \rho_b(t) x_i = a^{-3} E_{grav}(x_i, t) \ , \tag{14}$$

where $\rho_b(t)$ is the mean mass density at time t and

$$E_{grav}(x_i,t) = -2\pi G \sum_j m_j \mathrm{sign}(x_i - x_j) \ . \tag{15}$$

In an Einstein-de Sitter Universe we can make a nonlinear change of variable, $\tau = t_0 \log t/t_0$, such that (14) takes the form:

$$\frac{d^2x_i}{d\tau^2} + \frac{1}{3t_0}\frac{dx_i}{d\tau} - \frac{2}{3t_0^2}x_i = E_{grav}(x_i,\tau) \qquad \text{Q model} \ , \tag{16}$$

where $t_0^{-2} = 6\pi G\rho(t_0)$. This is the representation of the Vlasov-Poisson equations which we call the Quintic (Q) model.

The interest of this formulation is that, as for the classical static self-gravitating systems in one dimension, E_{grav} is a Lagrangian invariant, proportional to the net mass difference to the right and to the left of a given particle, at a given time. Hence, in between collisions, (16) has an explicit solution [1]:

$$x_i(\tau) = c_1^i \exp(\frac{2(\tau-\tau^n)}{3t_0}) + c_2^i \exp(-\frac{(\tau-\tau^n)}{t_0}) + K_i^n \ , \tag{17}$$

where $K_i^n = -(3t_0^2/2)E_{grav}(x_i,\tau)$, is constant. The coefficients c_1^i and c_2^i are determined by $x_i^n = x_i(\tau^n)$ and $w_i^n = \dot{x}_i(\tau^n)$, i.e. by the states of the particle at the time of the last crossing, and read:

$$\begin{cases} c_1^i = \dfrac{3}{5}\left[x_i^n + t_0 w_i^n - K_i\right] \\ \\ c_2^i = \dfrac{2}{5}\left[x_i^n - \dfrac{3}{2}t_0 w_i^n - K_i\right] \ . \end{cases} \tag{18}$$

The form of equation (17) suggests introducing an auxiliary variable $z = \exp((\tau-\tau^n)/3t_0)$. The crossing times between neighboring particles (i.e. i,$i+1$) can, hence, be computed by solving numerically the following *quintic* equation:

$$f(z) = A_{i,i+1}^n z^5 - B_{i,i+1}^n z^3 + C_{i,i+1}^n = 0 \ , \tag{19}$$

where:

$$\begin{cases} A^n_{i,i+1} = \dfrac{3}{5}\left[\Delta x^n_i + t_0 \Delta w^n_i - (K^n_{i+1} - K^n_i)\right] \\ \\ B^n_{i,i+1} = -(K^n_{i+1} - K^n_i) = const \\ \\ C^n_{i,i+1} = \dfrac{2}{5}\left[\Delta x^n_i - \dfrac{3}{2} t_0 \Delta w^n_i - (K^n_{i+1} - K^n_i)\right] , \end{cases} \tag{20}$$

and $\Delta x^n_i = x^n_{i+1} - x^n_i$, $\Delta w^n_i = w^n_{i+1} - w^n_i$. Thus, the evolution of the system is recovered by using a version of the event-driven scheme discussed in [20] and [11]. Details of the numerical implementation are given in [10].

Let as assume that in the interval L all the particles have equal mass $m_j = L\rho_0/N$. Then, the gravitational force in equation (16) transforms in

$$E_{grav}(x_i, \tau) = -\frac{L}{3Nt_0^2} \sum_j \text{sign}(x_i - x_j) = \frac{L}{3Nt_0^2} N_i \ . \tag{21}$$

where $N_i = N_{i,right} - N_{i,left}$ is the difference between the number of particles to the right and to the left of a given particle. At the initial time $\tau = \tau^0 = 0$, the positions of all the particles are ordered ($x_{i+1} > x_i$), and we have $N_i = N - (2i - 1)$. With K^0_i in the solution (17) constant we get

$$K^0_i = -\frac{L}{2N} N^0_i = -\frac{L}{2} + \frac{L}{N}(i - \frac{1}{2}) \ . \tag{22}$$

If we now pick the specific initial conditions such that all the c^i_2's in (17) are zero, we recover, in the discrete setting, the special case of correlated velocity and density perturbations, such that only the linearly increasing mode is excited. Note that this separation is valid until the first particle crossing, i.e. well into the non-linear regime. In this time interval we have

$$x_i(\tau) = \frac{3}{2} w^0_i t_0 \exp(\frac{2\tau}{3t_0}) - \frac{L}{2} + \frac{L}{N}(i - \frac{1}{2}) \ , \tag{23}$$

Hence, defining the new "time" $b = b_0 \exp(2\tau/3t_0)$ (with density dimension), the solution of (23) reduces to free motion of the particles. In other words, we have re-derived Zeldovich' approximation in the framework of the Q model.

In the Zeldovich approximation, this solution is assumed to hold for all time, even when the solution becomes multi-stream, while in the adhesion model we have merging of the particles after their crossing. The real system must necessarily lie somewhere in between.

4 A two particles system: an iterative map

Consider two particles of equal mass m interacting by the Q dynamics, confined in a box of size L. We choose units of length and mass such that $L = 1$ and $m = 1/2$. To streamline the following, we first first introduce the dimensionless variables:

$$\theta = \frac{\tau}{t_0} , \tag{24}$$

$$q_i(\theta) = \frac{x_i}{L} , \tag{25}$$

$$\beta_i(\theta) = \frac{6\dot{x}_i t_0}{L}. \tag{26}$$

Thus, before the time of first crossing, equation (17) takes the form:

$$q_i(\theta) = c_1^i \exp(\frac{2\theta}{3}) + c_2^i \exp(-\theta) \mp \frac{1}{4} . \tag{27}$$

where c_1^i and c_2^i are given by (18). We select a special class of initial condition: the velocities of the particles are arbitrarily assigned, while the positions are determined by setting c_2^i to zero (23). This simply means that there is no decaying mode initially, as discussed in the end of the previous section, and we can therefore immediately integrate the equations of motion of every particle up to its first crossing. In addition we chose a system of reference such that the center of mass is at rest at the origin. That means that the initial velocities are $w_1^0 = -w_2^0 > 0$. For simplicity we will suppress in the following the index i and consider the evolution of the leftmost of the two particles.

The time of first crossing, θ_{cross}, is then deduced from equation (27) and reads

$$\theta_{cross} = -\frac{3}{2} \ln \beta(0). \tag{28}$$

The rescaled particle's velocity is $\beta_{cross,0} = \beta(\theta_{cross}) = 1$. Remark that θ_{cross} is solely determined by the initial particle velocity, while $\beta_{cross,0}$ is a dimension-less constant, not dependent on the states of the particles at $\theta = 0$. This means that while the time at which the particles cross (θ_{cross}) depends on the initial velocity, their further evolution does not. On the other hand, after crossing the initial balance between positions and velocities no longer holds, and the condition $c_2^i = 0$ is no longer true. From that time on both the growing and decaying modes in (27) have to be considered in the analysis.

For times larger than θ_{cross}, the separation between the particles increases. Conversely, as an effect of the gravitational attraction, their velocities are progressively reduced. Hence, a turning point is reached where the elongation is maximal and the velocities are zero. The inversion time, θ_{turn}, follows by differentiating equation (17) with respect to time, and imposing the condition $\dot{q}(\theta_{turn}) = 0$. Thus:

$$\theta_{turn} = \theta_{cross} + \tilde{\theta} \tag{29}$$

where $\tilde{\theta} = \frac{3}{5}\ln 6$. The corresponding maximum elongation, $q_{max,0} = q(\theta_{turn})$, reads:

$$q_{max,0} = \frac{1}{4} - \frac{1}{5}6^{-\frac{3}{5}} - \frac{1}{20}6^{\frac{2}{5}} = \alpha \simeq 0.08. \tag{30}$$

It does not depend on the initial velocity.

Note that the particle inversion occurs before the *initial position* (i.e. $|q_i(0)| = \frac{1}{4}(1-\beta(0))$ is recovered: this is the effect of the friction-like term in equation (16), which is responsible for the progressive localization of the system around the center of mass. An analogous damping is shown to occur for the particles velocities. In fact, for $\theta > \theta_{turn}$, the particles move inward approaching the time of successive crossing. Due to the inner symmetry, the latter will take place in the origin. The particle rescaled velocity corresponding to the *first return* reads:

$$\beta_{ret} = \beta_{cross,1} = -0.83\beta_{cross,0} = -0.83. \tag{31}$$

By a simple generalization of the previous discussion, it can be shown that, for larger times, the particle executes damped oscillations. The particles move back and forth, displaying a progressive reduction of their mutual distance: the crossings become more frequent as time is increased. Take an index

n to label particle crossings in the system. The variable θ_n represents the time elapsed between the $n-1$'th and n'th crossings, and $\beta_{cross,n}$ is the dimensionless velocity of the particle at the n'th crossing. Then we make the further assumptions of smallness:

$$|\beta_{cross,n}| \ll 1. \tag{32}$$

For large enough n these are reasonable approximation. Further, we assume (32) to hold even for an early stage of the evolution: we will return on this point, and provide numerical support to the validity of this ansatz. Within these approximation the dynamics of (17) is reduced to the following simple map:

$$\begin{array}{lcl} \beta_{cross,n+1} & = & -\beta_{cross,n}\left(1-\frac{4}{3}\beta_{cross,n}\right) \\ \theta_{n+1} & = & 2|\beta_{cross,n}| \\ \Delta q_{max,n+1} & = & \frac{1}{12}\beta^2_{cross,n} \end{array} \tag{33}$$

where $\Delta q_{max,n}$ stands for the maximal elongation reached by the particles after n encounters. It is interesting that system (33) is actually equivalent to the motion of an impurity advected by an unsteady Burgers flow with a particular numerical relation between frictional and inertial forces, see [14].

Consider then the finite difference formula:

$$\frac{\Delta|\beta_{cross}|}{\Delta\theta} = \frac{|\beta_{cross,n+1}| - |\beta_{cross,n}|}{\theta_{n+1}}, \tag{34}$$

and rewrite the right hand-side using the first two relations of (33). Approximating the finite differences with differentials and integrating, using as initial condition for $|\beta_{cross}(\theta=\theta_{cross})|$ the velocity of at first crossing $|\beta_{cross,0}|$ and for $|\Delta q_{max}(\theta=\theta_{turn})|$ the first maximum elongation (30), one ends up with:

$$|\beta_{cross}(\theta)| = |\beta_{cross,0}| \exp\left(-\frac{1}{9}(\theta-\theta_{cross})\right), \quad \beta_{cross,0}=1, \tag{35}$$

$$|\Delta q_{max,0}(\theta)| = 2q_{max} \exp\left(-\frac{2}{9}(\theta-\theta_{turn})\right), \quad q_{max,0}=\alpha. \tag{36}$$

Here $|\beta_{cross}(\theta)|$ is the dimension-less velocity of the particles at the moment of their crossing and $\Delta q_{max}(\theta)$ the maximum separation between the two particles, at rescaled time θ. Both the velocity and the inter-particle distance

(and also the time elapsed between two successive crossing $\theta_n(\theta) \sim |\beta_{cross}(\theta)|$) decrease exponentially, as function of time θ, or, equivalently, a power-law decays is displayed in term of cosmological time t: $|\beta_{cross}(t)| \sim t^{-1/9}$ and $|\Delta q_{max}(t)| \sim t^{-2/9}$.

Let us turn to numerical simulations to test the reliability of our results. The initial condition is displayed in the small inset of Figure 1: here $c_2 = 0$, thus before the time of first crossing, only the contribution of the growing mode has to be considered. In the main plot of Figure 1 the absolute value of the particle velocity, β_{cross}, is represented as function of rescaled time θ, in scale lin-log. The solid line refers to the analytical prediction (35). In Figure 2 the particle maximum separation $\Delta q_{max}(\theta)$ is plotted versus θ, in linear-logarithmic scale (36). The solid line shows the theoretical result (36). In both case good agreement is displayed, even in the initial stage of the dynamics, thus confirming a posteriori the validity of our assumptions.

5 Density profile: Q model vs. adhesion model

The objective of this section is to investigate the density profile of a collapsing cluster in the Q model, and compare that to the adhesion model. We show that collapse in the Q model, which we recall is nothing but one-dimensional self-gravitating dynamics on the background of an Einstein-de Sitter Universe, is less pronounced. We derive a general expression for the density profile. To this end, we begin by analysing the motion a particle in an external halo, moving in the potential from a much more massive and very localized agglomeration. Then, we reconstruct the whole density distribution by combining together the contribution from each particle. These theoretical results are then compared first with numerical simulations of the Q model, and then with predictions based on the Zeldovich approximation and the adhesion model.

Consider a system of N particles of equal mass, confined in box of finite size $L = 1$, symmetric with respect to a reference point located at the origin. First, assume $N - 2l$ particles to form an inner bulk of width Δ, localized in the center of the box, with l much smaller than N, and Δ much smaller than L. The remaining $2l$ particles are assumed uniformly distributed in the

outer regions at the borders of the box.

To first approximation we can neglect the fine structure of the cluster, and replace it with an heavy, structure-less, *macro-particle*, carrying the same amount of mass. In addition, the gravitational interaction between the particles in the halo is also neglected. As a consequence, these particles are then not affected by the discreteness of the inner distribution: a sudden change in the acceleration is experienced when the origin is crossed.

As in the previous section, we set initial conditions such that only the growing mode is active, before the first particles crossing occurs, and use the same dimension-less variable. Consider the motion of particle i, situated to the left of the agglomeration and define:

$$\gamma_i = \frac{1}{2} - \frac{1}{N}(i - \frac{1}{2}) \ . \tag{37}$$

The positive parameter γ_i represents the absolute value of the initial position of the i'th particle ($w_i^0 = 0$ in (23)). In analogy with (28)-(31), one finds:

$$\theta_{i,cross} = -\frac{3}{2} \ln \left(\frac{\beta_i}{4\gamma_i} \right) \ , \tag{38}$$

$$\beta_{i,cross} = \beta_i(\theta_{cross}) = 4\gamma_i \ , \tag{39}$$

$$\theta_{i,turn} = \theta_{i,cross} + \tilde{\theta} \ = \theta_{i,cross} + \frac{3}{5} \ln 6 \ , \tag{40}$$

$$q_{i,max,0} = 4\alpha\gamma_i \ . \tag{41}$$

In this approximation, the i'th particle crosses for the first time the origin with rescaled velocity $\beta_{i,cross,0}$. Note that the latter is solely determined by the particle initial position. The corresponding maximum elongation $q_{i,max,0}$ is $4\alpha \simeq 0.32$ times smaller then the unperturbed distance γ_i.

By repeating the same procedure as in Section 4, one ends up with the following relations for, respectively, $|\beta_{i,cross}|$ and $|\Delta q_{i,max}|$:

$$|\beta_{i,cross}(\theta)| = 4\gamma_i \exp\left(-\frac{1}{9}(\theta - \theta_{i,cross}) \right) , \tag{42}$$

$$|\Delta q_{i,max}(\theta)| = 4\alpha\gamma_i \ \exp\left(-\frac{2}{9}(\theta - \theta_{i,turn})\right). \tag{43}$$

To validate our analysis we performed numerical simulations and studied the single particle behavior. In our experiments we considered the following initial condition: a finite, but large, fraction of all the particles, say $N - 2\ell$, is uniformly distributed in a narrow region, say Δ, centered around the reference origin. The remaining particles, ℓ of them, are symmetrically placed in the two lateral regions, with spatially uniform distribution. As a consequence, the inter-particle distance in the central bulk is smaller than in the external halos. In the limit when $\Delta \to 0$ and $\ell = 1$, we reach the conditions assumed in the preceding derivation. Velocities are given as a smooth function of positions.

In the upper panel of Figure 3 a phase space portrait of a single particle is represented: the damping, both in q and β, is clearly displayed. In the lower panel, the rescaled particle position q is plotted vs. time θ: the thin solid line refers to the simulation, while the thick curve is plotted from relation (43). Numerical simulations show good agreement with analytical predictions (42) and (43).

The previous results can also be extended to the case when particles are initially uniformly distributed in the finite size box. Given particle j, we neglect the interaction with the external masses (i.e. $|q_j| > |\gamma_i|$) and mimic the attraction of the inner particles by considering the forces exerted by a single massive object, localized in the origin. In this approximation, according to the lines of the preceding discussion, the behaviors of the $|\beta_{i,cross}(\theta)|$ and $|\Delta q_{i,max}(\theta)|$ are also described by equations (42) and (43). Despite the drastic assumptions involved, numerical simulations show relatively good agreement with theoretical predictions, provided the velocity distribution are smooth enough.

The goal of the remaining discussion is to derive an analytical estimate of the density profile by making use of these results. In the continuum limit ($N \to \infty$), the density $\rho(q, \theta)$ reads:

$$\rho(q, \theta) = \rho_0 / |\Delta q / \Delta\gamma|, \tag{44}$$

where we introduced the Jacobian of the transformation from Lagrangian

to Eulerian coordinates. The density field has a rather complex structure including singularities $\rho(q,\theta) \sim (q-q_m)^{-1/2}$, where q_m stands for the particle turning point. A rough characteristics of the cluster size, q_s, can be deduced from equation (41). In fact, before the time the outmost particle reaches, as the last one, the massive bulk, the size of the agglomeration, q_s, is given by:

$$q_s(\theta) = 4\alpha\gamma_{i*}(\theta) \ , \tag{45}$$

where $-\gamma_{i*}(\theta)$ is the initial coordinate of the particle which falls into the origin at the time $\theta - \tilde{\theta}$. From (38), (40) it follows:

$$\gamma_{i*}(\theta) = \frac{\beta_{i*}}{4} \exp\left(\frac{2}{3}(\theta - \tilde{\theta})\right) = \frac{\beta_{i*}}{6^{2/5}4} \exp\left(\frac{2}{3}\theta\right) \tag{46}$$

When the continuous limit is recovered, $\beta_{i*} = \beta(-\gamma_*)$, γ_* being the Lagrangian coordinate of the most periferic particle of the cluster, at time θ. Then assume that $\beta(-\gamma) \to 0$, as the edge of the box is approached ($\gamma \to 1/2$). Then from (46), γ_* tends to $1/2$, at large times, and consequently, from (45), $q_s(\theta) \to 2\alpha \simeq 0.16$. This observation on is in good agreement with the results of numerical simulations presented in a in previous work [10].

Inside the pancake a multistream flow has developed: the density at coordinate q follows by summing the contribution of each stream. Consider the *mean* density distribution assuming the length scale Δq much larger than the distance between two successive peaks i.e. larger than $|q_{m+1} - q_m|$. The sum can be then approximated by an integral over the Lagrangian coordinate γ. By introducing the density distribution function $f_\rho(\gamma,\theta)$ associated to the Lagrangian coordinate γ, we can write:

$$\rho(q,\theta) = \int_{\gamma_{min}}^{\gamma_{max}} f_\rho(\gamma,\theta) d\gamma. \tag{47}$$

Assume that all the particles belonging to a small Lagrangian interval, $\Delta\gamma$, are uniformly distributed inside the corresponding Eulerian segment $\Delta q_{max}(\theta,\gamma)$ (43):

$$\Delta q_{max}(\theta,\gamma) = |\Delta q_{i,max}(\theta)| = \frac{\chi\gamma^{\frac{4}{3}}}{\beta^{\frac{1}{3}}(\gamma)} \exp\left(-\frac{2}{9}\theta\right), \ \ \chi = 4^{4/3}6^{2/15}\alpha \tag{48}$$

and consider the mass conservation:

$$\rho_0 \Delta\gamma = \left(f(\gamma,\theta)\Delta\gamma\right) \Delta q_{max}(\theta,\gamma), \tag{49}$$

The interval $[\gamma_{min}(q,\theta), \gamma_{max}(\theta)]$ selects the particles that contributes to the density in q, at time θ. In particular they should have reached the origin, thus:

$$\frac{\beta(\gamma_{max})}{4} \exp\left(\frac{2}{3}\theta\right) = \gamma_{max}. \tag{50}$$

On the other hand the amplitudes of the particles' oscillations, $\Delta q_{max}(\theta,\gamma)$ have to be larger than q, thus γ_{min} is found by solving the following implicit equation.

$$q = \chi \exp\left(-\frac{2\theta}{9}\right) \frac{\gamma_{min}^{\frac{4}{3}}}{\beta^{\frac{1}{3}}(\gamma_{min})} \tag{51}$$

Finally, the density reads:

$$\rho(q,\theta) = \rho_0 \int_{\gamma_{min}}^{\gamma_{max}} \frac{d\gamma}{\Delta q_{max}(\theta,\gamma)} = \frac{\rho_0}{\chi} \exp\left(\frac{2}{9}\theta\right) \int_{\gamma_{min}}^{\gamma_{max}} \frac{\beta^{\frac{1}{3}}(\gamma)}{\gamma^{\frac{4}{3}}} d\gamma, \tag{52}$$

and $\rho(q,\theta) = 0$ when:

$$|q| > q_w(\theta) = \Delta q_{max}(\theta, \gamma_{max}). \tag{53}$$

Here $q_w(\theta)$ is the width of the mean density distribution. The density profile (52) depends on the initial particle velocity, namely $\beta(\gamma)$. In the following, we will solve analytically the integral in (52) for special class of initial conditions, and compare with numerics. In addition, we will discuss the analogous case in the adhesion model.

5.1 Step Profile of Initial Velocities

Assume the initial velocities profile to be given by:

$$\beta(q) = -\beta_0 \text{sign}(q), \tag{54}$$

where β_0 is a constant coefficient and, without loss of generality, we focus on the region $q > 0$.

First consider the evolution of the density in the Zeldovich approximation, with initial positions as in equation (23). Since the velocity profile at $\theta = 0$ is a step function, the particles with initial negative (resp. positive) spatial coordinate will move as a whole towards the origin, keeping their mutual distances constant. Thus before the last left particle reaches the origin, a two-stream flow develops over a finite region of width $2|q_{w,zeld}|$, where $|q_{w,zeld}| = \beta_0 \exp(2\theta/3)/4$. Note that the the density in each flow is equal to the initial density ρ_0.

Then follow the development under the Q dynamics later in time. By inserting (54) in (52) and performing the integral, one obtains:

$$\rho(q,\theta)|_{|q|<q_w} = \rho_0 \frac{3}{2q_p}\left[\left(\frac{q_p}{q}\right)^{1/4} - \left(\frac{1}{2\gamma_{max}}\right)^{1/3}\right], \tag{55}$$

where γ_{max} is solution of equation (50) and $q_p(\theta)$ is the spatial scale of inner structure

$$q_p = \frac{\chi}{2^{\frac{4}{3}}\beta_0^{\frac{1}{3}}} \exp\left(-\frac{2}{9}\theta\right). \tag{56}$$

We recall that $q_w(\theta)$ stands for the width of the pancake, see eq. (53). Consider also the mass function $M(q,\theta)$:

$$M(q,\theta) = \int_0^q \rho(\xi,\theta)\ d\xi, \tag{57}$$

Inserting eq. (55) and performing the integral one ends up with:

$$M(q,\theta) = \rho_0 \left[2\left(\frac{q}{q_p}\right)^{3/4} - \frac{3}{2}\left(\frac{1}{2\gamma_{max}}\right)^{1/3}\left(\frac{q}{q_p}\right)\right]. \tag{58}$$

In the initial stage of the evolution $\beta(\gamma_{max}) = \beta_0$, thus, from equation (50):

$$\gamma_{max} = \frac{\beta_0}{4} \exp\left(\frac{2}{3}\theta\right). \tag{59}$$

The pancake's density distribution is therefore characterized by two length scales: the spatial scale of inner structure, $q_p(\theta)$, which decays exponentially, see (56), and the width of the agglomeration which grows exponentially according to:

$$q_w(\theta) = \frac{\chi\beta_0}{4^{\frac{1}{3}}} \exp\left(\frac{2}{3}\theta\right) \simeq 0.1\beta_0 \exp\left(\frac{2}{3}\theta\right). \tag{60}$$

It is worth stressing that during the initial stage of the pancake's formation, the width q_w increases with time slower than as predicted in the Zeldovich picture. From equation (55) it follows that the density in the bulk increases exponentially in time-like coordinate θ, according to $\rho(q,\theta) \sim q^{-(1/4)} \exp(\theta/6)$. In other words, the system tends to display a progressively denser core, localized near the origin. The mass contained in the cluster is also increasing exponentially, $m_p(\theta) = 2M(q_w,\theta) = \rho_0\beta \exp(2\theta/3)/2$, in agreement with the predictions of the Zeldovich model. The discussion above applies to the co-moving frame, but physical density is measured in the inertial frame; the two are related by (1). We will return to this point in Sect. 7. Let us however in brief state that the collapse in co-moving coordinates is slower than the expansion of the Universe. The physical density therefore on the contrary decreases at around almost all mass points, and in an inertial coordinate system the agglomerations spread out over time, albeit more slowly than the expansion of the Universe as a whole.

Equations (58)-(60) suggest that, initially, both the mean density distribution and mean mass function are self-similar. In particular:

$$M(q,\theta) = m_p \left[2\left(\frac{q}{q_w}\right)^{3/4} - \frac{3}{2}\left(\frac{q}{q_w}\right)\right] = m_p(\theta)\overline{M}(q/q_w(\theta)). \tag{61}$$

In the very late time evolution of an isolated cluster all particles have reached the inner bulk (i.e. $\theta > -3/2\ln(\beta_0/2)$). The box length, L, is normalized to one so that, $m_p(\theta) = \rho_0$. Then $\gamma_{max} = 1/2$ and equations (55),(57) indicate the a self-similar collapse:

$$M(q,\theta) = \overline{M}(q/q_p(\theta)). \tag{62}$$

Now both the density and the mass function are solely characterized by a unique length scale, which is both the inner length scale, $q_p(\theta)$, and the outer

length scale, q_w. In this case q_p is the coordinate of the out-most particle, and the density for $q > q_p$ is identically equal to zero.

Summing up, we have shown that for an initial condition in the form of equation (54), the mean mass function $M(q,\theta)$, displays a self-similar collapse, in different stages of the evolution. Introducing the rescaled variable $x = q/q_w(\theta)$, the function $\overline{M}(q/q_w(\theta))$ takes the universal form:

$$\overline{M}(x) = \left[2x^{3/4} - \frac{3}{2}x\right]. \tag{63}$$

for $x = [0,1]$, where $\overline{M}(1)$ is equal to one half. From (63) it follows that the matter is mainly concentrated around the pancake center. In particular, one-half of the whole mass (i.e. $2\overline{M}(x_{0.5}) = 1/2$) is found to lay in a symmetric interval defined by $x_{0.5} = 0.14$, while 90% of it, is distributed in a segment equal to half the size of entire cluster ($x_{0.9} = 0.54$).

To validate our theoretical analysis we now turn to numerical simulations and consider the late stage of evolution of an initial perturbation in the form (54). The particles are initially uniformly distributed in space. In Figure 4 the normalized density profile is plotted at late stage of evolution (thin solid line) and superposed to the theoretical prediction (55) (thick solid line). The same curves are represented in scale log-log in the left inset: here the circles refer to the simulation. No parameter need to be adjusted by numerical fitting and the agreement has to be considered satisfying. The corresponding phase space portrait is reported in the right inset of Figure 4, where the characteristic spiral behavior is clearly displayed. In figure 5 the cumulative mass function is plotted as a function of the variable $\xi = q/q_p$.

In a previous work of two of the authors, [10], we studied the late time evolution of an isolated perturbation within the framework of the Q dynamics. In particular we measured the progressive contraction of the inner region of the agglomeration, when compared to the overall Universe expansion. This effect was computed by the width of region, Δq_μ, that contains a fraction μ of the whole mass of the system, centered around the position of maximum density. It turned out that the interval Δq_μ shrinks in time according to a power-law of cosmological time t, with exponent $-2/9$. An heuristic interpretation was also provided in [10]. To make a bridge between our present investigations and these earlier findings we define q_μ (63) such that $2M(q_\mu,\theta) = \rho_0\mu = const$. From equation (62) it follows that Δq_μ

scales proportionally to q_p; thus we are led to assume $q_\mu = x_\mu q_p$, where x_μ is a positive coefficient. Equation(56) implies:

$$q_\mu = \frac{\chi x_\mu}{2^{\frac{4}{3}}\beta_0^{\frac{1}{3}}} \exp\left(-\frac{2}{9}\theta\right) \tag{64}$$

in qualitative agreement with the results in [10]. As an example, let us focus on the case $\mu = 1/2$. In this case, $x_\mu = 0.14$. We performed numerical simulations starting with the same class of initial condition as in Figure 4. In Figure 6, $q_{1/2}$ is plotted vs. θ: circles refer to the numerical simulation and the solid line represents equation (64). The slopes of the two curves in figure 6 agree, but the amplitudes do not. We can make the difference smaller by adjusting some of the hypotheses made in the derivation above. In particular, we considered the particles belonging to the cluster to be uniformly distributed in the finite interval Δq_{max} given by (48). In reality, the particles spend more time on the border. This effect is explicitly modeled by assuming:

$$q_{p,eff} = cq_p \tag{65}$$

where c is an "ad hoc" numerical factor, larger than one.

To complete this section, let us compare our theoretical expression (55) with the density profile derived in the framework of the adhesion model. These results, which we recall in the following, are detailed in [12]. Let as consider the stationary solution of Burgers equation :

$$v(x,b) = v_{st}(x) = -U\tanh\left(\frac{x}{\delta}\right), \tag{66}$$

where $\delta = U/2\nu$ is the width of the shock. This solution is also the asymptotic solution of Burgers equation for the initial the step-function profile previously considered. The trajectories of individual particles $x(b)$ satisfy the following equation

$$\frac{dx(b)}{db} = v(x,b), \tag{67}$$

where the field $v(x,b)$ is determined by the solution of the Burgers equation. Assuming that $v(x,b)$ is a stationary solution of Burgers equation from (66),(67) we have the following expression for the coordinates of the particles

$$x(b,y) = \delta \mathrm{Arc}\sinh\left[\sinh(y/\delta)\exp(-Ub/\delta)\right] \tag{68}$$

where y stands for the Lagrangian coordinate. From the conservation of mass, the following expression for the density is derived:

$$\rho(x,b) = \frac{\rho_0 \cosh\left(\frac{x}{\delta}\right)}{\sqrt{\sinh^2\left(\frac{x}{\delta}\right) + \exp\left(\frac{-2Ub}{\delta}\right)}}, \tag{69}$$

Solutions (68) do not apply to the intermediate stage of evolution. Thus we will focus on the asymptotic behavior, for time $b \gg \delta/U$ and consider the regions $|x| > \delta_p$, where $\delta_p = \delta \exp(-Ub/\delta)$. The particles in the agglomeration behave according to

$$x(b,y) = y \exp(-Ub/\delta). \tag{70}$$

Thus in the adhesion model a faster collapse is displayed, when compared to the exact Q dynamics: in the latter a power-law decay in "Burgers time" b, is in fact produced, namely $q_p(b,y) = y(b/b_0)^{-1/3}$. As concern the density profile, for $x < \delta_p$, one gets:

$$\rho(x,b) = \frac{\rho_0 \exp\left(\frac{Ub}{\delta}\right)}{\sqrt{1 + \left(\frac{x^2}{\delta^2}\right)\exp\left(\frac{2Ub}{\delta}\right)}}, \tag{71}$$

hence maximum value of the density increases exponentially in "Burgers time", $\rho_{max}(0,b) = \rho_0 \exp(Ub/\delta)$. In the interval $\delta_p \ll x \ll \delta$ the density transforms into a time-independent power-law distribution

$$\rho(x,b) = \rho_0 \frac{\delta}{x} = \rho_0 \frac{2\nu}{Ux}. \tag{72}$$

Thus in the adhesion model we have that the asymptotic density distribution for the initial step profile is localized in the regions $|x| < \delta = const$, has non-integrable time independent power law tails (72) with cutoff scale $\delta_p = \delta \exp(-Ub/\delta)$. In the Q model we have instead an integrable power-law distribution, see (55).

When considering a perturbation in a finite box, in co-moving coordinates, both the Quintic and the adhesion models show the formation of a dense structure. However, in the adhesion model, the width q_p of the pancake decreases faster ($g_p \sim \exp -b$) then in Q-model ($g_p \sim b^{-1/3}$).

These discrepancies suggest that, at least in one dimension, the adhesion approach is valid only as an approximate model of structure formation. This observation agrees with the conclusion in [10] where a new transport equation was proposed.

6 Interaction of two massive clusters

In this section we consider the dynamics of two interacting clusters. As a first approximation, one can neglect the inner discrete structure of a cluster, by introducing a single *macro-particle* to mimic its dynamics. Thus, the problem is first reduced to the study of the evolution of a two particles system, investigated in Section 4. According to this picture, the agglomerations move back and forth displaying damped oscillation. This observation agrees with previous numerical investigations reported in [9]. Following the discussion of the previous section, each massive agglomeration experiences a contraction of the inner core: the competition of these two effects determines the late-time asymptotics of the system.

Numerical simulation are performed starting with the initial condition displayed in Figure 7 a). The distance between the two centers of mass, δ, is plotted vs. time θ, in Figure 7 c). The damping tendency is evident (thin solid line) and the theoretical prediction (36) (thick solid lines) agrees with the numerical findings. At late time the two clusters still present a finite separation, see 7 b). This is in a good agreement with the theoretical predictions of Sections 4 and 5.1, both the widths of the agglomerations and amplitude of their mutual oscillations decay as the same exponential function of time, hence their ratio is a constant number. Therefore, the system composed by two interacting clusters, with finite inner structure, evolves approximately in a self-similar way.

7 Concluding remarks

In this paper we considered the problem of structure formation in a Einstein-de Sitter Universe, focusing on planar perturbations. This was done by using the Q model, or Quintic model, a Lagrangian representation previously derived in [1], in which one of the steps is to solve a large number of quintic

equations. We underline however that the Q model is nothing but the motion of a system of gravitationally interacting particles, on the background of an expanding Universe, with convenient choices of time and space coordinates. We showed that the Q model can be approximated by an even simpler iterative map. This observation permitted to establish a connection with [14] where the motion of turbulent flows with strong friction was analyzed, and to derive theoretical predictions for both the density profile and the mass function in a collapsing cluster. These predictions were cross-validated with direct numerical simulation.

The main conclusion of this work is that the inner structure of a Zeldovich pancake is different from the adhesion model, with finite viscosity in the Burgers equation. That there is a discrepancy is what one would expect, but this had nevertheless to our knowledge never been shown before. As a mathematical problem, a qualitative difference is that in co-moving coordinates, the size of collapsing cluster goes down as power-law with cosmological time in the self-gravitating system, but as a stretched exponential in the adhesion model [1]. As a physical problem, the difference is even more dramatic: in the self-gravitating system the characteristic scale of the density distribution is given in co-moving coordinates by equation (56), which decreases, with cosmological time t, as $(t/t_0)^{-\frac{2}{9}}$. The co-moving system of coordinates is related to an inertial system by equation (1), where the proportionality is $(t/t_0)^{\frac{2}{3}}$. Combining the two, the characteristic scale of a collapsing cluster hence *increases* in time, as $d(t) \sim (t/t_0)^{\frac{4}{9}}$. Since the density distribution of equation (55) is self-similar, the maximum density attained depends on the graininess of the initial conditions. We have not investigated the law of the increase of the maximum density, but it is at least possible that with continuous initial density distributions arbitrarily high densities can be produced, also if measured in an inertial system of reference. A more interesting characteristics is however the fraction of total mass M where (in an inertial system) the density is higher than some cut-off ρ_{cr}. That quantity scales as $\left(\frac{M}{\rho_{cr} d(t)}\right)^3$. Since $d(t)$ is an increasing function of time in the inertial system, that fraction decreases as $(t/t_0)^{-\frac{4}{3}}$. In this sense one-dimensional self-gravitating motion, on the background of an expanding Universe, is not effective in bringing about

[1] In "Burgers time" the collapse is simply exponential, see subsection 5.1.

mass collapse.

In the adhesion model the characteristic scale decreases, both in a co-moving and an inertial system. Here both the maximum real-space density and the fraction of mass at a density larger than some cut-off *increases*. The adhesion model is therefore, in contrast, effective in bringing about mass collapse in one dimension. In other words, the adhesion model over-predicts the clustering tendency, and overestimates the peak density. A Universe in which most mass lies in regions where density decreases can never give rise to galaxies, galaxy clusters and other significant objects. The analysis given here therefore suggests, quantitatively, why a one-dimensional description of mass agglomeration is insufficient.

We have also investigated the mutual motion of two pancakes, and shown them to be closely similar to the decaying oscillations of two mutually attracting "heavy particles".

8 Acknowledgements

This work was mainly supported by a grant from the Swedish Royal Academy of Sciences (KVA), further support from the Swedish Research Council through grants NFR F 650-19981250 (D.F) and NFR I 510-930 (E.A.), and RFBR (02-02-17374, 00-15-96619) and "Universities of Russia" (S.N.G. and A.Yu.M) is also gratefully acknowledged. E.A. thanks the Edwin Schrödinger Institute (Vienna) for hospitality, and for opportunities to discuss and write up this work. D.F. thanks Ph. Choquard for enlighting discussions. We thank A. Noullez for fruitful discussions.

References

[1] Aurell E. & Fanelli D., cond-mat/0106444 (2001)

[2] *BOOMERANG Home Page*, http://www.physics.ucsb.edu/∼boomerang/ .

[3] Buchert T. & Domínguez A., *A&A* , **335**, 395 (1999).

[4] Buchert T., Domínguez A. & Perez-Mércader, *A&A* , **349**, 343 (1999).

[5] Caldwell R.R., Dave R. & Steinhardt P.J., *Phys. Rev. Lett.* **80** 1582 (2001).

[6] *COBE Home Page*, http://www.gsfc.nasa.gov/astro/cobe/ /cobe_home.html.

[7] *DMR images* This web site includes qualitative color-coded pictures of the anisotropies in the Cosmic Background Radiation field as observed by the COBE satellite, as well as down-loadable data sets, http://www.gsfc.nasa.gov/astro/cobe/dmr_image.html.

[8] Doroshkevich A.G., Kotok E.V., Novikov I.D., Poludov A.N., Shandarin S.F. & Si gov Yu.S. at al. 1980, *MNRAS*,**192**, 321

[9] Fanelli D., TRITA-NA-0209, NADA, KTH, Stockholm, Sweden

[10] Fanelli D., Aurell E., *Astronomy & Astrophysics* (2002) [in press].

[11] Fanelli D., Aurell E. & Noullez A., Proceeding of IAU Symposium 208 (2001).

[12] Gurbatov S.N., Proceedings of the International school of physics "E. Fermi", Course CXXXII, Dark Matter in the Universe, Societá Italiana di Fisica,645-660,1996.

[13] Gurbatov S.N., Malakhov A.N., Saichev A.I. *Nonlinear Random Waves and Turbulence in Nondispersive Media: Waves, Rays, Particles* (Manchester University Press, 1991).

[14] Gurbatov S.N., Mainardi F., Moshkov A.Yu., Tampieri F. Izvestia VUZov:PND, Saratov, 4-5 (2002)

[15] Gurbatov S.N., Saichev A.I. & Shandarin S.F. 1989, *MNRAS*, **236**, 385.

[16] Harrison E.R., *Phys. Rev. D* **1** (1970) 2726-2730.

[17] Kamionkowsky M. & Kosowsky A., *Ann. Rev. Nucl. Part. Sci.* **49** (1999) 77-123.

[18] Lifshitz E., J. Phys. USSR, **10**, 116 (1947).

[19] *MAP Home Page*, http://map.gsfc.nasa.gov/ .

[20] Noullez A., Fanelli D. & Aurell E., submitted to Journ. Comp. Phys., cond-mat/0101336 (2001).

[21] Peebles P.J. , The Large-scale Structure of the Universe, (Princeton University Press, Princeton, NJ) (1980).

[22] Press, H.W., Numerical Recipes in Fortran, (Cambridge University Press, Cambridge) (1992).

[23] Rouet J.L., Feix M.R. & Navet M., Vistas in Astronomy, **33**, 357 (1990).

[24] Rouet J.L. et al., in Lecture Notes in Physics: Applying Fractals in Astronomy, 161 (1991).

[25] Shandarin S.F. & Zeldovich Ya.B., Rev. Mod. Phys., **61**, 185 (1989).

[26] Tegmark M., *Science* **296** 1427-1433 (2002).

[27] Yano T.& N.Gouda N., *The astrophysical Journal. Suppliment Series* **118** 267 (1998).

[28] Vergassola M., Dubrulle B., Frisch U. & Noullez A., *A&A*, **289**, 325 (1993).

[29] Weinberg S., Gravitation and Cosmology (Wiley) (1972).

[30] Weinberg S., *Phys. Rev. D* **64** (2001) 123511.

[31] Weinberg S., *Phys. Rev. D* **64** (2001) 123512.

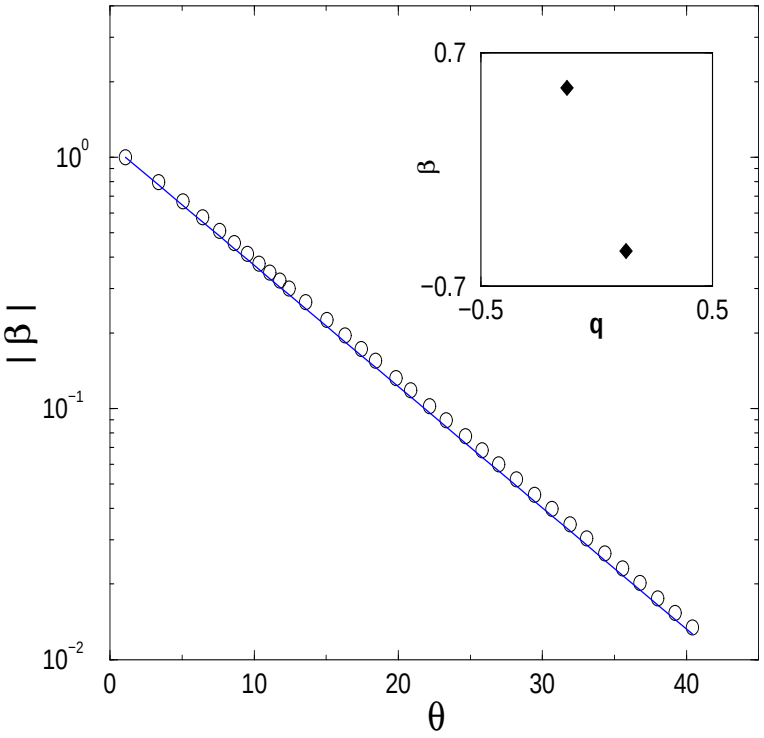

Figure 1: The absolute value of the velocity β_{cross} is plotted as function of rescaled time θ, in scale lin-log. Circles refer to the simulations, while the solid line is the theoretical prediction (35). The initial condition is displayed in the small inset.

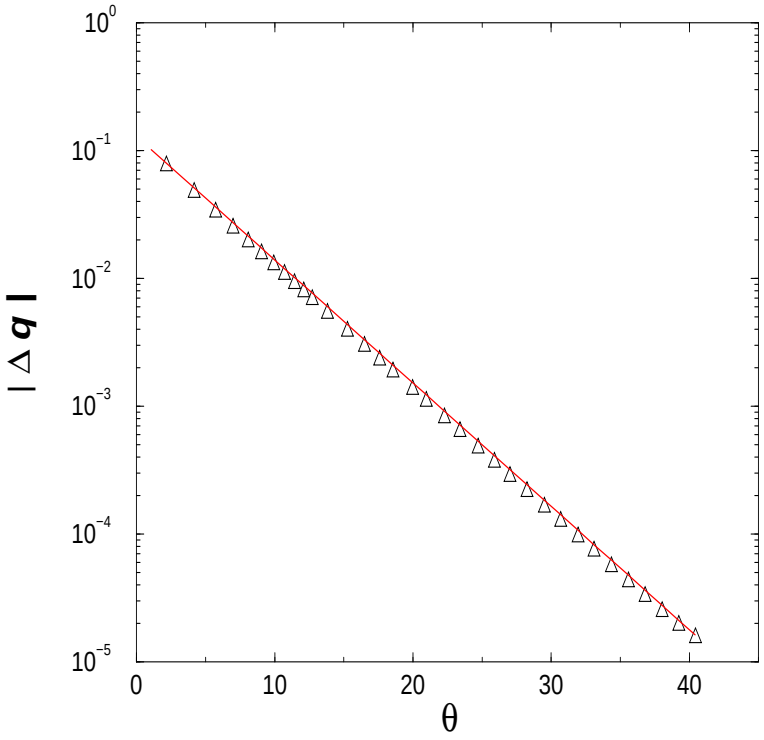

Figure 2: *The inter-particle distance $|\Delta q_{max}|$ is represented as function of rescaled time θ, in scale lin-log. Triangles refer to the simulation, while the solid line is the theoretical prediction (36).*

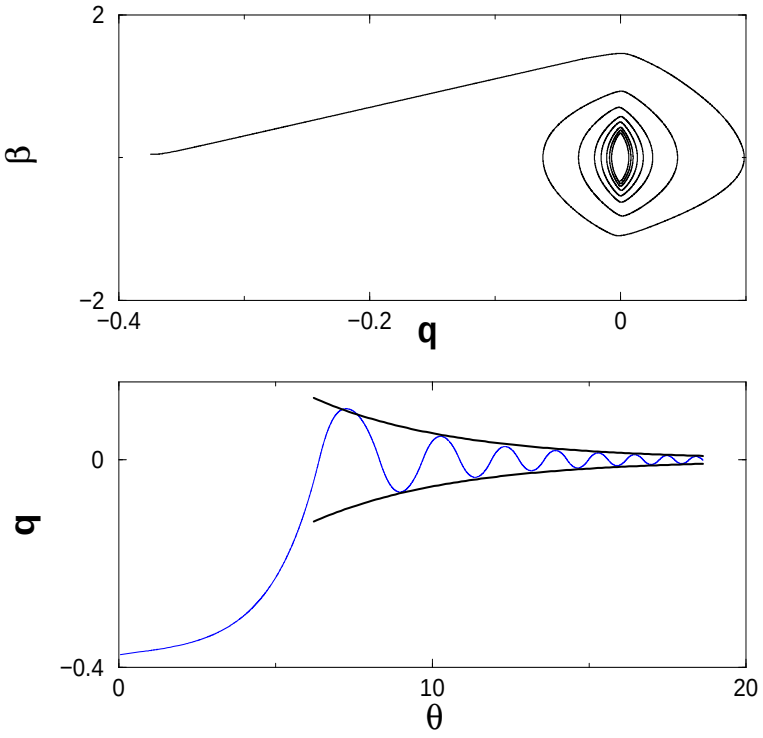

Figure 3: *Upper panel: phase space portrait of a single particle. Lower panel: position q vs. rescaled time θ. The thin solid line refers to the simulation while the thick curve represent the theoretical prediction (43). No parameter needs to be adjusted by numerical fitting. Here* $N = 1024$, $N - 2\ell = 768$, $\Delta = 0.15$.

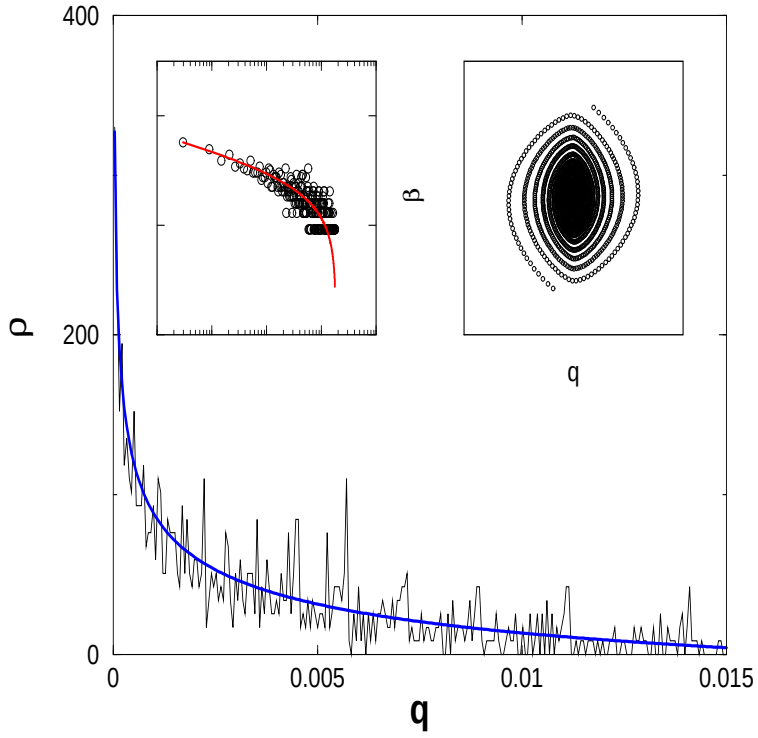

Figure 4: *Main plot: normalized density profile ρ vs. at late stage of evolution rescaled position q, starting from a step-profile for velocities. The particles are initially uniformly distributed in space. The thin solid line refers to the simulation, while the thick solid one represents the theoretical prediction (55)($\gamma_{max} = 1/2$). In this case $N = 2000$, $\theta = 23.27$, $\beta_0 = 4.9 \times 10^{-4}$. Hence, $q_p = 0.0183$. Left inset: normalized density profile ρ vs. rescaled position q in log-log scale. The circles refer to the simulation. Right inset: phase space portrait at $\theta = 23.27$.*

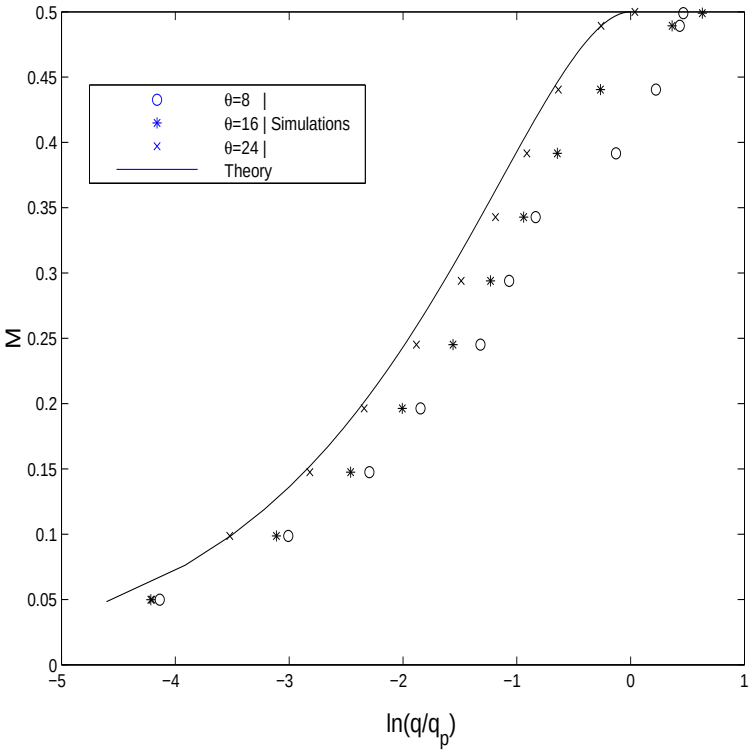

Figure 5: *Mass function $M(q,\theta)$ in lin-log scale vs. normalized coordinate q/q_p. The particles are initially distributed uniformly in space, velocity a step-function of position. The thick solid line represents the theoretical prediction (58)($\gamma_{max} = 1/2$). The circles, stars and crosses refer to the simulation at different times.*

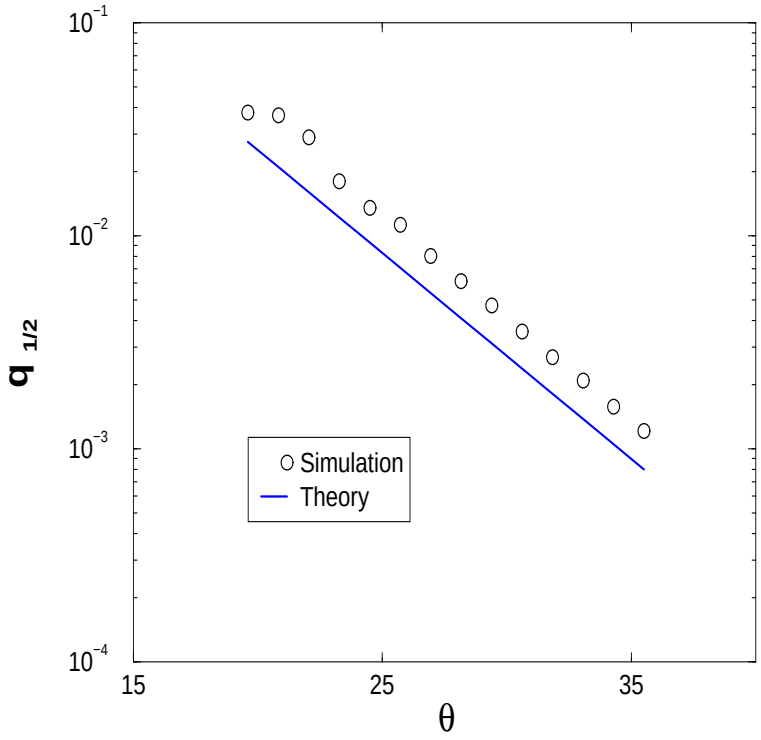

Figure 6: *$q_{1/2}$ is plotted vs. θ. The circles represent the results of the numerical experiment. The solid line refers to the theoretical prediction (equation (64)).*

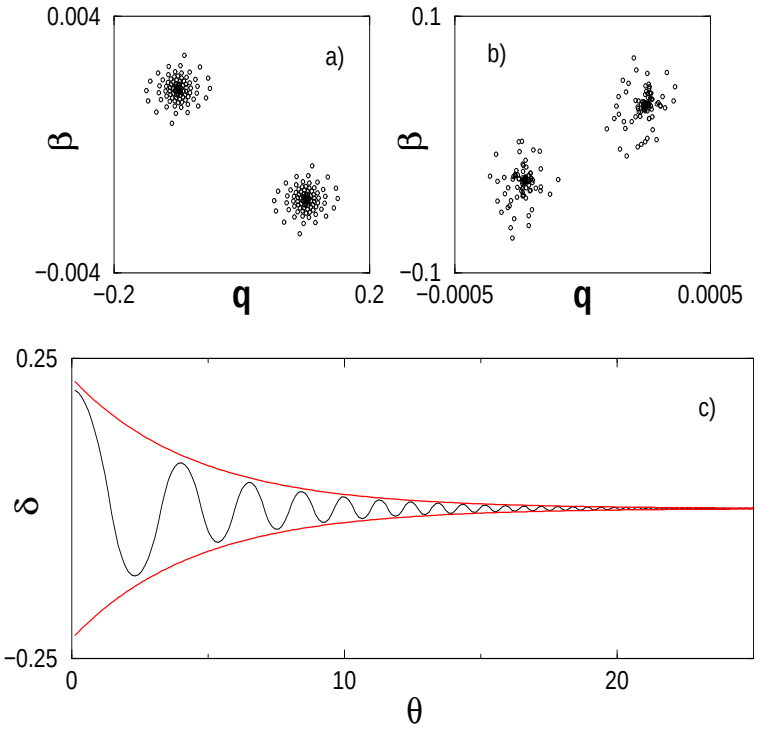

Figure 7: *Figure a): Initial phase space portraits. Here* $N = 200$. *Figure b): Phase space portrait at time* $\theta = 25.5$. *Figure c):* δ *vs. rescaled time* θ. *The thin solid line refers to the simulation. The thick curves represent eq. (36). Here* $\theta_{cross} = 1.38$.